Journal of Solid State Chemistry **152,** 211–220 (2000)
doi:10.1006/jssc.2000.8684, available online at http://www.idealibrary.com on IDEAL®

Structural Properties and Topological Diversity of Polymeric Ag(I)-hexamethylenetetramine Complexes: Self-Assembly of Three Novel Two-Dimensional Coordination Networks and Their Supramolecular Interactions

Lucia Carlucci,* Gianfranco Ciani,†,[1] Davide M. Proserpio,† and Silvia Rizzato†

*Dipartimento di Biologia Strutturale e Funzionale, Universita' dell'Insubria, Via J. H. Dunant 3, 21100 Varese, Italy; and
†Dipartimento di Chimica Strutturale e Stereochimica Inorganica, Centro CNR, Via G. Venezian 21, 20133 Milano, Italy

The self-assembly of polymeric open networks from different Ag(I) salts and the potentially tetradentate ligand hexamethylenetetramine (hmt) has revealed a variety of possible structural motifs, depending on the reagent ratios and the counterions, that are discussed in comparison. Three new Ag(I) coordination polymers are here described, *namely* $[Ag_2(\mu_4\text{-hmt})(Tos)_2]$ (Tos = *p*-toluenesulfonate) (1), $[Ag_2(\mu_3\text{-hmt})_2(CF_3SO_3)(H_2O)](CF_3SO_3)\cdot H_2O$ (2), and $[Ag_3(\mu_3\text{-hmt})_2(H_2O)_4](PF_6)_3$ (3), that contain two-dimensional infinite layers of different types. Crystal data: 1 $C_{20}H_{26}Ag_2N_4O_6S_2$, monoclinic, $C2/c$, $Z = 4$, $a = 9.482(3)$ Å, $b = 8.539(3)$ Å, $c = 28.461(10)$ Å, $\beta = 91.75(2)^\circ$, $V = 2303.3(13)$ Å^3, $R = 0.043$ ($I > 2\sigma(I)$); 2 $C_{14}H_{28}Ag_2F_6NO_8S_2$, monoclinic, $P2_1/c$, $Z = 4$, $a = 6.429(2)$ Å, $b = 25.247(3)$ Å, $c = 16.162(2)$ Å, $\beta = 91.54(2)^\circ$, $V = 2622.4(9)$ Å^3, $R = 0.050$ ($I > 2\sigma(I)$); 3 $C_{12}H_{32}Ag_3F_{18}N_8O_4P_3$, monoclinic, $C2/c$, $Z = 4$, $a = 16.675(4)$ Å, $b = 11.102(5)$ Å, $c = 18.455(3)$ Å, $\beta = 111.48(2)^\circ$, $V = 3179.2(17)$ Å^3, $R = 0.040$ ($I > 2\sigma(I)$). Compound 1 is composed of layers of square grids, with the silver ions acting as spacers and interacting with the anions through Ag–O contacts and also via π bonds with the aromatic rings. Compound 2 consists of layers of hexagons, with alternate triconnected Ag(I) ions and tridentate hmt ligands, while compound 3 contains layers of larger hexagonal meshes, with six hmt ligands at the vertices and six biconnected silver atoms as spacers. The latter two species give rise, *via* hydrogen-bond bridges involving coordinated water molecules, to three-dimensional arrays of new topologies. © 2000 Academic Press

Key Words: **structure; extended framework; coordination polymer; silver(I); hexamethylenetetramine.**

INTRODUCTION

The deliberate design of new nanoporous materials based on polymeric coordination compounds (1), of interest for their potential properties in molecular selection, ion exchange, and catalysis, requires the use of suitably tailored building blocks. Different strategies have been employed, involving either coordinative interactions [with neutral (2) or anionic (3) ligands] or hydrogen bonding (4). In the former case the use of polydentate bases of suitable geometry [trigonal (5), square planar (6), tetrahedral (1a,7)] introduces into the frameworks also organic centers in addition to the metallic ones, which can give rise to new and variated topological types. It is also possible that polydentate ligands assembled with digonal metal centers (*L–M–L* metallic synthons, like biconnected silver ions) can entirely dictate the topology of the array (8). In this concern the self-assembly of the potentially tetradentate ligand hexamethylenetetramine (hmt) with the coordinatively versatile silver ions can produce interesting architectures, paralleling the supramolecular organic chemistry of adamantyl templates with different synthons (9, 10). Some possible target structural motifs for Ag–hmt systems are those illustrated in Scheme 1, which include the hexagonal layers I and II and the supertetrahedral networks III and IV. Indeed, super-diamond frames like III and IV have been observed in two species containing the related adamantanoid cage anion $(Ge_4S_{10})^{4-}$, *namely* in $[Mn(Ge_4S_{10})](NMe_4)_2$ (11) and $[Cu_2(Ge_4S_{10})](NEt_4)_2$ (12), respectively. Also wurtzite-like nets can be considered as target structures, taking into account that Ermer has recognized this topology in the hydrogen bonded network of the $[NH_4(hmt)](BF_4)$ adduct (13).

Working on these lines we have reacted hmt with different Ag(I) salts of poorly coordinating anions under different conditions and we have already reported on many novel networks, showing interesting topologies (14–17). Though no supertetrahedral species was isolated, we have continued our investigations in order to get more information on these systems and we report here on three novel polymeric

[1] To whom correspondence should be addressed. Fax. +39-0270635288. E-mail: davide@csmtbo.mi.cnr.it.

0022-4596/00 $35.00

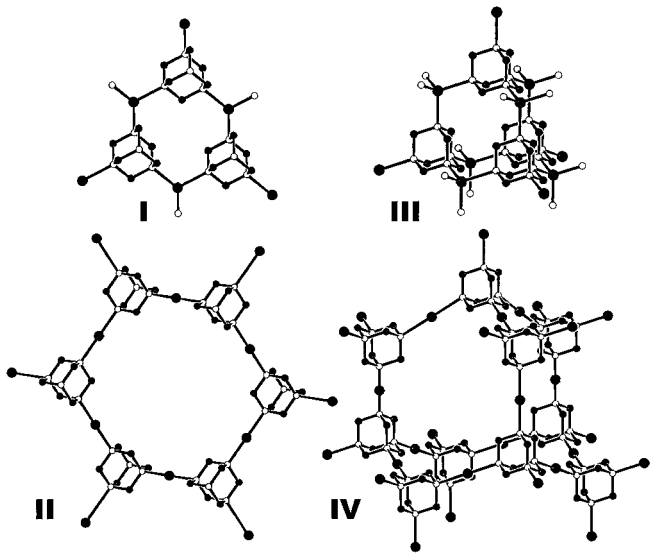

SCHEME 1

species, *namely* $[Ag_2(\mu_4\text{-hmt})(Tos)_2]$ (Tos = *p*-toluenesulfonate) (**1**), $[Ag_2(\mu_3\text{-hmt})_2(CF_3SO_3)(H_2O)](CF_3SO_3)\cdot H_2O$ (**2**), and $[Ag_3(\mu_3\text{-hmt})_2(H_2O)_4](PF_6)_3$ (**3**), containing different types of infinite layers that form extended three-dimensional architectures via supramolecular interactions, like π–π stackings or hydrogen bonds. A survey of all the structural motifs as yet found for Ag–hmt systems is also reported, with a brief comparative discussion.

EXPERIMENTAL

All the reagents and solvents employed were commercially available high- purity materials (Aldrich Chemicals), used as supplied, without further purification. Elemental analyses were carried out at the microanalytical laboratory of this university. IR spectra were collected on a Perkin-Elmer FT-IR Paragon 1000 spectrometer. Thermal analyses were performed on DSC 7 and TGA 7 Perkin-Elmer instruments with a heating rate of 10°C/min under nitrogen flux. X-ray powder diffraction spectra were collected on a Philips PW 1820 vertical-scan diffractometer.

Synthesis of $[Ag_2(\mu_4\text{-}hmt)(Tos)_2]$ (*Tos = p-toluenesulfonate*) (**1**). Compound **1** was obtained by layering over a solution of hexamethylenetetramine (0.040 g; 0.28 mmol) in CH_2Cl_2 (3 ml) a solution of silver tosylate (0.78 g, 0.28 mmol) in CH_3CN (3 ml). The solution was left for some days in the dark, affording a white powder which was recovered by filtration, washed with CH_2Cl_2, and dried in the air (yield ca. 80%). The nature of this material as pure **1** was confirmed by X-ray powder diffraction data compared with the spectrum calculated from the single-crystal X-ray structure. Single crystals of **1**, suitable for structural analysis, were obtained by slow evaporation of more diluted solutions of the metal salt and hmt in molar ratio 1 : 1. Anal. Calcd. for $C_{10}H_{13}AgN_2O_3S$: C, 34.40; H, 3.75; N, 8.02. Found: C, 34.62; H, 3.68; N, 7.80. Main IR bands in Nujol mull: 1593w, 1232s, 1213s, 1166s, 1118s, 1025s, 1003vs, 811s, 680s cm^{-1}. TGA analysis of **1** shows a weight loss starting at 230°C (ca. 60%), the residue being mainly metallic silver as evidenced by X-ray powder diffraction.

Synthesis of $[Ag_2(\mu_3\text{-}hmt)_2(CF_3SO_3)(H_2O)](CF_3SO_3)\cdot H_2O$ (**2**). On a solution of hexamethylenetetramine (0.0622 g, 0.44 mmol) in CH_2Cl_2 (4 ml) we have layered a solution of $AgCF_3SO_3$ (0.114 g, 0.44 mmol) in ethanol (4 ml). The solution, left to slowly evaporate for many days in the dark, gave a white precipitate of **2**, which was filtered, washed with ethanol, and dried in the air (yield $> 80\%$). The white powder was confirmed as pure **2** by X-ray powder diffraction data compared with the spectrum calculated from the single-crystal X-ray structure. Small needle-shaped colorless single crystals of **2**, suitable for structural analysis, were obtained by slow evaporation of more diluted solutions of $AgCF_3SO_3$ and hmt in molar ratio 1 : 1. Anal. Calcd. for $C_7H_{14}AgF_3N_4O_4S$: C, 20.25; H, 3.40; N, 13.50. Found: C, 20.82; H, 3.10; N, 13.80. Main IR bands in Nujol mull: 3517s, 3472s, 1631w, 1223vs, 1193s, 1174s, 1023vs, 1004vs, 988vs, 799s, 695s, 643s cm^{-1}. TGA analysis of **2** shows a weight loss of 4%, corresponding to the water content, in the range 70–160°C, and then starts to decompose at 200°C. On heating up to 600°C the residual sample is mainly metallic silver as evidenced by X-ray powder diffraction.

Isolation of $[Ag_3(\mu_3\text{-}hmt)_2(H_2O)_4](PF_6)_3$ (**3**). Compound **3** has been isolated as a minor product from the reaction of $AgPF_6$ in *i*-propanol with hmt in CH_2Cl_2 in molar ratio of 2 : 1. Slow evaporation (almost to dryness) of these mixtures gave few flat colorless crystals of **3**, together with a dominant amount of the already described species $[Ag(hmt)](PF_6)\cdot H_2O$ (**14**). The nature of **3** has been established by single crystal X-ray analysis.

Crystallography. Colorless crystals of compounds **1–3** were mounted at room temperature (293 K) under a coating of cyanoacrilic glue on an Enraf-Nonius CAD-4 diffractometer, and 25 intense reflections having a θ value in the range 9.0–12.0° were centered using graphite-monochromated Mo$K\alpha$ radiation ($\lambda = 0.71073$ Å). Least-squares refinement of their setting angles resulted in the unit-cell parameters reported in Table 1. Crystal data and details associated with data collections and structure refinements are also given in Table 1. An ω-scan mode was used with a scan interval of 1.1° for **1** and 0.8° for **2** and **3**, with a θ range of 3–25° for all species. Intensities were checked by monitoring three standard reflections every 3 h; a decay of 2.5% was observed for **1**, while no significant crystal decay

TABLE 1
Crystallographic Data and Structure Refinement for Compounds 1–3

Compound	**1**	**2**	**3**
Empirical formula	$C_{20}H_{26}Ag_2N_4O_6S_2$	$C_{14}H_{28}Ag_2F_6N_8O_8S_2$	$C_{12}H_{32}Ag_3F_{18}N_8O_4P_3$
Formula weight	698.31	830.30	1110.98
Crystal system	Monoclinic	Monoclinic	Monoclinic
Space group	$C2/c$ (No.15)	$P21/c$ (No. 14)	$C2/c$ (No. 15)
Unit cell dimensions	$a = 9.482(3)$ Å	$a = 6.429(2)$ Å	$a = 16.675(4)$ Å
	$b = 8.539(3)$ Å	$b = 25.247(3)$ Å	$b = 11.102(5)$ Å
	$c = 28.461(10)$ Å	$c = 16.162(2)$ Å	$c = 18.455(3)$ Å
	$\beta = 91.75(2)^\circ$	$\beta = 91.54(2)^\circ$	$\beta = 111.48(2)^\circ$
Volume	2303.3(13) Å^3	2622.4(9) Å^3	3179.2(17) Å^3
Z	4	4	4
Density (calculated) (g/cm^3)	2.014	2.103	2.321
Absorption coefficient (mm^{-1})	1.928	1.752	2.124
F (000)	1392	1648	2160
θ-Range for data collection	3–25°	3–25°	3–25°
Index ranges	$-11 \le h \le 11$, $0 \le k \le 10$, $0 \le l \le 33$	$-7 \le h \le 7$, $0 \le k \le 29$, $0 \le l \le 19$	$-19 \le h \le 18$, $0 \le k \le 13$, $0 \le l \le 21$
Reflections collected	2066	4595	2766
Independent reflections	2026 [R(int) = 0.0293]	4595 [R(int) = 0.0000]	2765 [R(int) = 0.0231]
Data/restraints/parameters	2026/0/155	4595/61/251	2765/55/218
Goodness-of-fit on F^2	1.175	0.976	1.049
Obs. refl. criterion	$I > 2\sigma(I)$	$I > 2\sigma(I)$	$I > 2\sigma(I)$
Final R indices[a,b]	$R1 = 0.0435$, $wR2 = 0.0860$	$R1 = 0.0503$, $wR2 = 0.1089$	$R1 = 0.0398$, $wR2 = 0.1027$
R indices (all data)	$R1 = 0.1071$, $wR2 = 0.0957$	$R1 = 0.2275$, $wR2 = 0.1439$	$R1 = 0.0788$, $wR2 = 0.1149$
Weighting parameters, a, b[c]	0.0226, 13.633	0.0619, 0.0	0.0603, 17.7018
Largest diff. peak and hole	0.666 and -0.571 eÅ^{-3}	1.410 and -1.365 eÅ^{-3}	0.948 and -0.808 eÅ^{-3}

[a] $R1 = \sum \| F_o| - |F_c \| / \sum |F_o|$,
[b] $wR2 = [\sum w (F_o^2 - F_c^2)^2 / \sum w F_o^4]^{1/2}$.
[c] Weighting: $w = 1/[\sigma^2(F_o^2) + (aP)^2 + bP]$, where $P = (F_o^2 + 2F_c^2)/3$.

was observed in **2** and **3**. The diffracted intensities were corrected for Lorentz, polarization, decay, and background effects. An empirical absorption correction was applied, based on ψ-scans of three suitable reflections having χ values close to 90° (ψ 0–360°, every 10°). The structures were solved by a combination of direct methods (SIR97) (18) and difference Fourier methods and refined by full-matrix least-squares on F_o^2, using all reflections. One of the PF_6^- anions in **3**, lying in a special position on a twofold axis, was found disordered and was refined using a model involving two octahedra sharing the same apical $F(21)$ atoms and with double equatorial fluorines of different weight, centered on the unique P atom. Anisotropic thermal displacement parameters were assigned to all nonhydrogen atoms in **1** and **3** (except for the four disordered fluorines), and only to the Ag atoms and the triflate anions in **2**. The hydrogen atoms were located on calculated positions and introduced in the final stages of refinement as fixed atom contributions riding on their parent atoms. All calculations were performed using SHELXL-97 (19). Final atomic coordinates for compounds **1–3** are given in Tables 2–4. Molecular drawings were produced with the SCHAKAL-97 program (20).

RESULTS AND DISCUSSION

Our previous investigations on the self-assembly of hmt and the salts $AgPF_6$ (14–16), $AgSbF_6$ (15), and $AgClO_4$ (17) have revealed some trends in this chemistry: (i) the reactions lead often to mixtures of derivatives and the first product formed (favoured by kinetic factors) can give further reactions on standing in the solution; (ii) the counterions, the molar ratio of the reagents, and the solvent system play a fundamental role in orienting the self-assembly; (iii) the silver ions show a variety of coordination modes and the hmt ligands can behave as bidentate, tridentate, or tetradentate. All these factors make quite difficult any project of deliberate design of networked materials. Nevertheless, the interesting structural results already obtained and the hope of getting a better insight into the self-assembly of these systems have prompted us to attempt reactions of hmt with other silver salts, containing larger counterions, as *p*-toluenesulfonate (tosylate) and triflate.

Silver *p*-toluenesulfonate has been reacted at room temperature with hmt in different ratios, from 2:1 to 1:1, in CH_3CN/CH_2Cl_2 affording in all cases as unique product the polymeric compound $[Ag_2(\mu_4\text{-hmt})(Tos)_2]$ (**1**). The

TABLE 2
Atomic Coordinates and Equivalent Isotropic Displacement Parameters (Å^2) for 1

	x	*y*	*z*	*U*(eq)
Ag	0.25821(5)	0.50553(9)	0.32589(2)	0.03780(18)
S	0.5083(2)	0.7980(3)	0.13884(7)	0.0393(5)
O(1)	0.4664(9)	0.9242(8)	0.1098(3)	0.091(3)
O(2)	0.6494(6)	0.8126(10)	0.1569(3)	0.095(3)
O(3)	0.4107(9)	0.7676(9)	0.1742(3)	0.106(3)
C(14)	0.5078(8)	0.6263(9)	0.1038(2)	0.0351(18)
C(15)	0.3834(9)	0.5550(10)	0.0920(3)	0.047(2)
C(16)	0.3798(11)	0.4204(12)	0.0650(3)	0.060(3)
C(17)	0.5031(13)	0.3542(11)	0.0497(3)	0.063(3)
C(18)	0.6310(11)	0.4295(11)	0.0616(3)	0.059(3)
C(19)	0.6327(9)	0.5653(10)	0.0877(3)	0.048(2)
C(110)	0.5017(14)	0.2048(12)	0.0215(4)	0.090(4)
N(1)	0.0863(6)	0.8605(6)	0.2187(2)	0.0286(14)
N(2)	− 0.0946(5)	0.6560(6)	0.2200(2)	0.0284(13)
C(5)	− 0.0074(7)	0.7582(9)	0.1905(2)	0.0292(17)
C(6)	0.0000	0.5589(11)	0.2500	0.029(2)
C(7)	0.0000	0.9579(10)	0.2500	0.028(2)
C(8)	0.1795(6)	0.7572(8)	0.2491(2)	0.0279(16)

product is air and light stable for long times and almost insoluble in the common organic solvents. Thermal analyses (DSC and TGA) have shown that the polymeric network is stable up to ca. 230°C and starts to decompose at this temperature after an exothermic peak.

In a similar way we have prepared compound **2** by reacting silver triflate in ethanol with hmt in CH_2Cl_2, using different molar ratios. The product precipitates as very small needle-shaped crystals. As for **1**, we have ascertained the pure nature of the bulk product by X-ray powder diffraction methods. The thermal behavior of **2** is similar to that of other previously reported Ag–hmt polymeric species containing solvated water molecules that lose endothermically the water content at $T < 160$°C and start to decompose above 200°C after an exothermic peak (14, 17).

Further investigations on the reactivity of $AgPF_6$, that has already afforded four different Ag–hmt species, have also been carried out under variated reaction conditions. A solution of the silver salt in *i*-propanol was reacted with hmt in CH_2Cl_2 in the molar ratio 2 : 1. Evaporation almost to dryness gave as main product the already known compound $[Ag(hmt)](PF_6)\cdot H_2O$ (14). Examination under the microscope of samples of the product revealed the presence of few crystals of a new species, identified by single crystal X-ray analysis as $[Ag_3(\mu_3\text{-hmt})_2(H_2O)_4](PF_6)_3$ (**3**). Unfortunately we have been unable to find a synthetic route for **3** or to get more information on this species.

The structural investigations have revealed that all these compounds are polymeric species and are discussed below. Selected bond distances and angles for **1–3** are given in Table 5.

Structure of $[Ag_2(\mu_4\text{-}hmt)(Tos)_2]$ (*Tos = p-toluenesulfonate*) (**1**). The crystal structure of **1** consists of two-dimensional undulated $[Ag_2(\mu_4\text{-hmt})]$ layers of square meshes, with four-connected hmt ligands at the nodes of the framework and the silver ions acting only as spacers (see Fig. 1). Considering the rigid tetrahedral bonding geometry of the hmt ligands, the square grid can be obtained thanks only to the nonlinear coordination at the Ag(I) ions. The metal atoms coordination sphere is highly distorted tetrahedral, involving two N atoms of two hmt molecules, one oxygen atom of an anion, and a η^1-bonded aromatic ring of another close anion. This π interaction of silver [Ag–C 2.688(8) Å]

TABLE 3
Atomic Coordinates and Equivalent Isotropic Displacement Parameters (Å^2) for 2

	x	*y*	*z*	*U*(eq)
Ag(1)	− 0.23809(13)	0.14836(3)	0.26308(5)	0.0335(2)
Ag(2)	0.25736(14)	0.33236(3)	0.08968(5)	0.0353(2)
N(11)	0.7531(14)	0.3816(3)	− 0.0958(5)	0.0271(19)
N(12)	0.9469(13)	0.3706(3)	0.0356(5)	0.027(2)
N(13)	0.7546(14)	0.4521(3)	0.0066(5)	0.032(2)
N(14)	0.5646(13)	0.3704(3)	0.0319(5)	0.027(2)
C(11)	0.9404(15)	0.3586(4)	− 0.0536(6)	0.027(2)
C(12)	0.5671(16)	0.3592(4)	− 0.0586(6)	0.029(2)
C(13)	0.7523(18)	0.4398(4)	− 0.0813(7)	0.035(3)
C(14)	0.9412(18)	0.4290(4)	0.0474(7)	0.040(3)
C(15)	0.7551(15)	0.3479(4)	0.0706(6)	0.027(2)
C(16)	0.5680(17)	0.4289(4)	0.0439(7)	0.032(3)
N(21)	0.2559(12)	0.2424(3)	0.1175(5)	0.0234(19)
N(22)	0.2472(13)	0.1521(3)	0.0624(5)	0.030(2)
N(23)	0.4516(12)	0.1707(3)	0.1884(5)	0.0251(19)
N(24)	0.0674(12)	0.1720(3)	0.1915(5)	0.0244(18)
C(21)	0.4483(16)	0.2272(4)	0.1666(6)	0.029(2)
C(22)	0.0751(16)	0.2291(4)	0.1685(6)	0.030(3)
C(23)	0.2484(17)	0.2085(4)	0.0429(6)	0.033(3)
C(24)	0.4348(17)	0.1393(4)	0.1107(6)	0.036(3)
C(25)	0.0669(17)	0.1399(4)	0.1129(6)	0.034(3)
C(26)	0.2625(16)	0.1589(4)	0.2379(6)	0.031(3)
O(1W)	0.3323(16)	0.3598(4)	0.2272(6)	0.075(3)
O(2W)	0.2480(18)	0.4645(4)	0.8277(7)	0.093(3)
S(1)	0.7086(5)	0.21642(11)	− 0.11879(17)	0.0346(7)
O(11)	0.7415(11)	0.2256(3)	− 0.0328(4)	0.0380(19)
O(12)	0.4974(11)	0.2090(4)	− 0.1438(4)	0.055(2)
O(13)	0.8188(13)	0.2512(3)	− 0.1698(5)	0.062(3)
C(1)	0.8311(18)	0.1519(5)	− 0.1353(6)	0.055(4)
F(11)	1.0299(13)	0.1541(4)	− 0.1165(5)	0.102(4)
F(12)	0.8094(14)	0.1378(4)	− 0.2122(5)	0.105(4)
F(13)	0.7507(19)	0.1157(3)	− 0.0893(7)	0.134(4)
S(2)	0.2536(6)	− 0.00495(13)	− 0.2127(2)	0.0561(10)
O(21)	0.186(2)	0.0379(3)	− 0.2578(7)	0.137(6)
O(22)	0.4735(17)	− 0.0147(8)	− 0.2189(10)	0.220(10)
O(23)	0.144(2)	− 0.0521(4)	− 0.2243(7)	0.149(7)
C(2)	0.226(2)	0.0106(5)	− 0.1037(10)	0.125(9)
F(21)	0.321(2)	0.0545(5)	− 0.0854(8)	0.176(7)
F(22)	0.284(2)	− 0.0264(4)	− 0.0563(6)	0.180(7)
F(23)	0.028(2)	0.0198(6)	− 0.0930(9)	0.201(8)

TABLE 4
Atomic Coordinates and Equivalent Isotropic Displacement Parameters (Å²) for 3

	x	*y*	*z*	*U*(eq)
Ag(1)	0.16872(4)	0.40668(5)	0.73132(3)	0.0446(2)
Ag(2)	0.0000	0.0000	0.5000	0.0464(2)
N(1)	0.2558(3)	0.0485(4)	0.6812(3)	0.0256(10)
N(2)	0.1881(3)	0.2473(4)	0.6628(3)	0.0263(10)
N(3)	0.1204(3)	0.0848(4)	0.5710(3)	0.0295(11)
N(4)	0.2539(3)	0.1750(5)	0.5727(3)	0.0293(11)
C(1)	0.2377(4)	0.1566(5)	0.7198(3)	0.0274(12)
C(2)	0.1727(4)	− 0.0034(5)	0.6305(3)	0.0288(12)
C(3)	0.3039(4)	0.0875(6)	0.6310(3)	0.0292(13)
C(4)	0.1052(3)	0.1923(5)	0.6127(3)	0.0286(13)
C(5)	0.2368(4)	0.2795(5)	0.6122(4)	0.0320(14)
C(6)	0.1724(4)	0.1217(6)	0.5236(3)	0.0327(14)
O(1W)	0.0253(4)	− 0.4865(7)	0.6836(4)	0.084(2)
O(2W)	0.0890(5)	0.2949(7)	0.8125(4)	0.091(2)
P(1)	0.13148(14)	− 0.34204(18)	0.53850(11)	0.0519(5)
F(11)	0.1140(4)	− 0.2224(5)	0.4883(3)	0.0859(17)
F(12)	0.0717(7)	− 0.2912(8)	0.5780(6)	0.173(4)
F(13)	0.1931(5)	− 0.3893(7)	0.4983(4)	0.112(2)
F(14)	0.1463(6)	− 0.4581(5)	0.5909(4)	0.117(2)
F(15)	0.2102(5)	− 0.2774(5)	0.6014(3)	0.109(2)
F(16)	0.0547(5)	− 0.4023(7)	0.4734(5)	0.147(3)
P(2)	0.0000	− 0.0803(3)	0.7500	0.0577(8)
F(21)	− 0.0237(5)	− 0.0769(14)	0.6615(4)	0.210(7)
F(22A)[a]	− 0.0976(7)	− 0.0301(12)	0.7265(7)	0.082(5)
F(23A)[a]	− 0.0869(8)	− 0.1347(16)	0.7474(8)	0.098(5)
F(22B)[a]	− 0.0319(14)	0.0454(14)	0.7650(14)	0.179(10)
F(23B)[a]	− 0.0467(15)	− 0.2042(17)	0.7456(14)	0.191(9)

[a] SOF for F(22A), F(23A) = 0.473(15); for *F*(22B), *F*(23B) = 0.527(15).

falls within the limits observed in many recently reported Ag–aromatic complexes (21). In each square mesh two anions are disposed in such a way to cross-link the silver ions on the opposite edges, as shown in Fig. 1 (bottom), forming a small adamantane-like cage.

Similar two-dimensional $[Ag_2(\mu_4\text{-hmt})]$ square layers are present in the recently reported species $[Ag_2(\mu_4\text{-hmt})(SO_4)(H_2O)]\cdot 4H_2O$ (22), containing two nonequivalent Ag(I) spacers, with trigonal and T-shaped coordination geometries. Both polymeric species can be described as layers of tetrahedra sharing four vertices, but with different configurations (see Fig. 2), which can be referred to the prototypical structures of HgI_2 (red) and $SrZnO_2$, respectively, according to Wells (23a).

The layers of **1** stack along the crystallographic *c* axis, with a separation of 1/2 *c* [14.23 Å (Fig. 3)]. The aromatic rings of the anions of each layer show π–π interactions with the rings in the adjacent (upper and lower) layers (stacking distance 3.7 Å, offset 2.2 Å).

Structure of $[Ag_2(\mu_3\text{-}hmt)_2(CF_3SO_3)(H_2O)](CF_3SO_3)\cdot H_2O$ (**2**). The crystal structure of **2** consists of two-dimensional infinite $[Ag(\mu_3\text{-hmt})]$ layers of hexagonal meshes, formed by alternate three-connected hmt ligands and silver ions (Fig. 4). The layers are markedly undulated as schematically shown in Fig. 5. This 2D motif is common to other Ag–hmt polymers, like $[Ag(\mu_3\text{-hmt})](NO_3)$ (24) and $[Ag(\mu_3\text{-hmt})](ClO_4)$ (17), though different conformations of the six-membered rings are observed, due to the variable coordination geometries at the Ag(I) centers, which range from trigonal to tetrahedral, depending on the presence of weak bonds with the anions or with solvent molecules. In **2** there are two different types of silver ions: Ag(1) shows an essentially trigonal environment, involving the N atoms of three hmt ligands (Ag–N mean 2.387 Å), but presents an additional longer contact with one oxygen atom of a triflate [Ag–O 2.585(10) Å], while Ag(2) is distorted tetrahedral, with three Ag–N(hmt) bonds (mean 2.366 Å) and one Ag–O(H_2O) bond [2.365(10) Å].

It is noteworthy that the coordinated water molecules give hydrogen bonds with the coordinated anions belonging to adjacent layers (O···O 2.76 Å). A three-dimensional (3, 4-connected) network is thus generated by these Ag–O(H_2O)···O(triflate)–Ag bridges. We have previously reported that intercalation between the layers of $[Ag(\mu_3\text{-hmt})](ClO_4)$ of additional Ag(I) ions, acting as spacers that

TABLE 5
Selected Bond Lengths (Å) and Angles (°) for 1–3

		Compound **1**	
Ag–N(1)	2.331(5)	N(1)–Ag–N(2)	113.68(19)
Ag–N(2)	2.374(5)	N(1)–Ag–O(3)	89.1(2)
Ag–O(3)	2.587(8)	N(2)–Ag–O(3)	91.7(2)
Ag–C(19)	2.688(8)	N(1)–Ag–C(19)	111.5(2)
		N(2)–Ag–C(19)	128.8(2)
		O(3)–Ag–C(19)	111.8(3)
		Compound **2**	
Ag(1)–N(23)	2.372(8)	N(23)–Ag(1)–N(24)	112.7(3)
Ag(1)–N(24)	2.382(8)	N(23)–Ag(1)–N(11)	121.1(3)
Ag(1)–N(11)	2.406(8)	N(24)–Ag(1)–N(11)	125.5(3)
Ag(1)–O(23)	2.585(10)	N(23)–Ag(1)–O(23)	107.5(4)
Ag(2)–N(21)	2.316(7)	N(24)–Ag(1)–O(23)	85.2(3)
Ag(2)–N(12)	2.364(8)	N(11)–Ag(1)–O(23)	86.9(3)
Ag(2)–O(1W)	2.365(10)	N(21)–Ag(2)–N(12)	117.7(3)
Ag(2)–N(14)	2.407(8)	N(21)–Ag(2)–O(1W)	96.1(3)
O(1W)···O(21)	2.762(13)	N(12)–Ag(2)–O(1W)	112.1(3)
O(2W)···O(22)	2.596(18)	N(21)–Ag(2)–N(14)	118.3(3)
		N(12)–Ag(2)–N(14)	112.8(3)
		(1W)–Ag(2)–N(14)	95.7(3)
		Compound **3**	
Ag(1)–N(2)	2.265(5)	N(2)–Ag(1)–N(1)	141.36(17)
Ag(1)–N(1)	2.276(5)	N(2)–Ag(1)–O(1W)	118.9(2)
Ag(1)–O(1W)	2.522(6)	N(1)–Ag(1)–O(1W)	97.5(2)
Ag(1)–O(2W)	2.648(7)	N(2)–Ag(1)–O(2W)	98.8(2)
Ag(2)–N(3)	2.170(5)	N(1)–Ag(1)–O(2W)	100.7(2)
O(1W)···O(1W)	2.868(13)	O(1W)–Ag(1)–O(2W)	79.0(2)
O(1W)···O(2W)	3.102(12)	N(3)–Ag(2)–N(3)	180.0
O(2W)···O(2W)	3.019(14)		

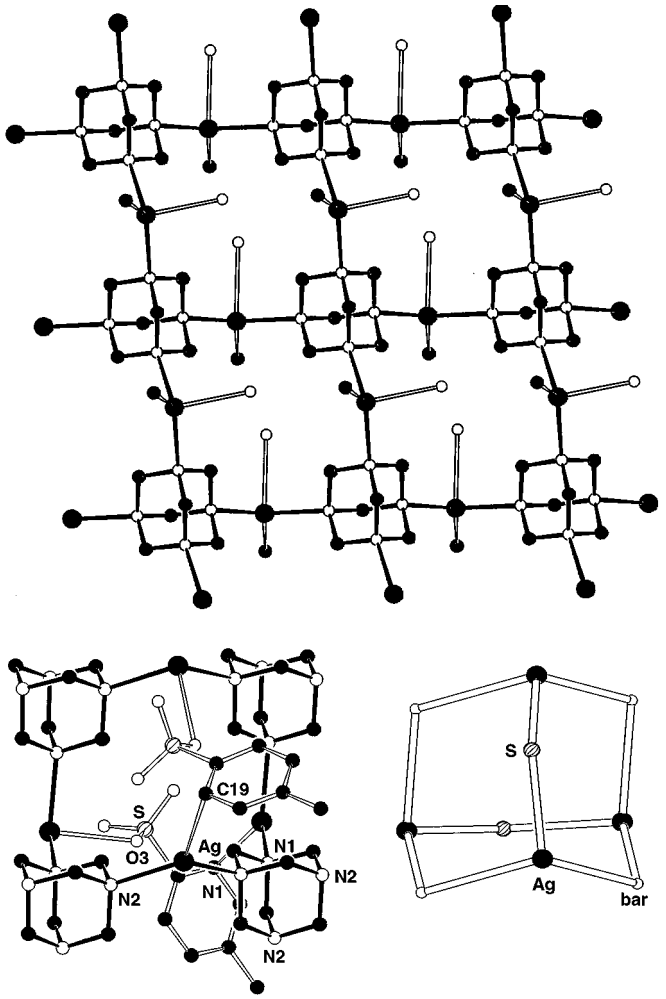

FIG. 1. A view of a two-dimensional layer in **1** (top) and a single square mesh with the bridging anions (bottom left) forming an adamantanoid cage (schematized at bottom right; bar, baricenters of the hmt molecules).

join the layers, leads to a tridimensional (3,4)-connected open framework with $(6^3)(6^5,8)$-b topology (17). In **2** hydrogen bonding plays a similar role in connecting the layers but the resulting topology, schematically shown in Fig. 6, is more complex [(3,4)-connected tetranodal] with three-connected hmt and four-connected silver atoms. The channels are occupied by the uncoordinated anions and by solvated water molecules.

Structure of $[Ag_3(\mu_3\text{-}hmt)_2(H_2O)_4](PF_6)_3$ (**3**). Also the structure of compound **3** is composed of two-dimensional layers of hexagonal meshes, but at difference from **2**, each hexagon presents six three-connected hmt ligands at the vertices, joined by six two-connected silver ions acting only as spacers (see Fig. 7). The hexagonal edges are, therefore, quite longer than in **2** (on average 7.17 Å vs 3.87 Å). There are two different types of silver ions: Ag(2) shows a symmetry imposed digonal coordination with two hmt ligands

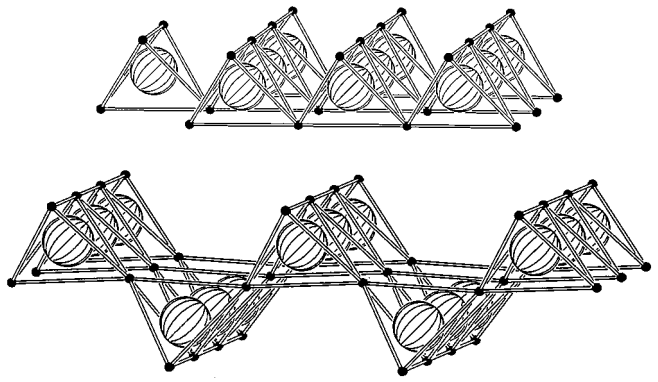

FIG. 2. Schematic views of the layers of tetrahedra sharing four vertices in compound **1,** of the HgI_2 type (top), and in $[Ag_2(\mu_4\text{-}hmt)(SO_4)(H_2O)]\cdot 4H_2O$ (22), of the $SrZnO_2$ type (bottom). Black small spheres represent silver atoms and big shaded spheres stand for the htm molecules.

[Ag–N 2.170(5) Å], while Ag(1) is four-coordinated, to two N atoms of hmt ligands [mean Ag–N 2.270 Å, N–Ag–N 141.36(17)°] and two water molecules (mean Ag–O 2.585 Å). This difference is mainly responsible of the marked deviation from planarity of the layers, that can also be described as a system of parallel helical chains, hmt–Ag(1)–hmt–Ag(1)–hmt, extending along the *b* crystallographic axis, joined together by the Ag(2) spacers.

The layers are interconnected via hydrogen bonds involving the coordinated water molecules, as shown in Fig. 8. The resulting 3D three-connected array is schematically

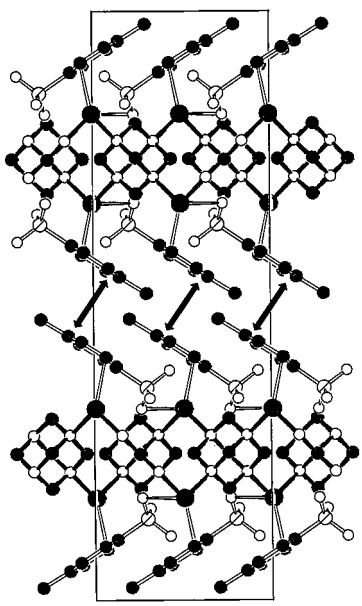

FIG. 3. Crystal packing of **1** down the *a* axis showing the stacking of the aromatic rings of the anions of adjacent layers.

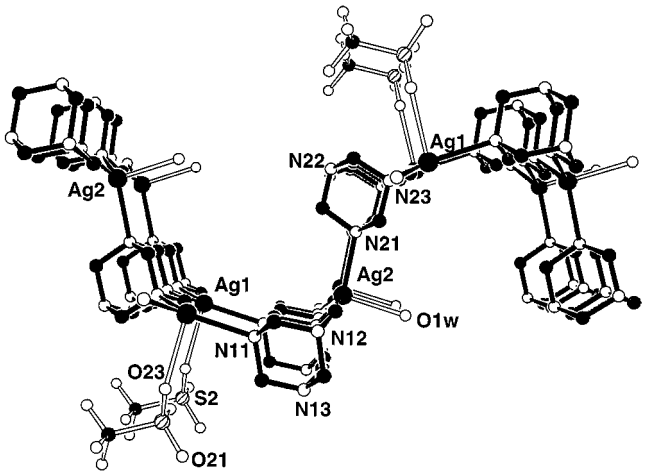

FIG. 4. A lateral view of an undulated layer of **2,** with partial atomic labeling.

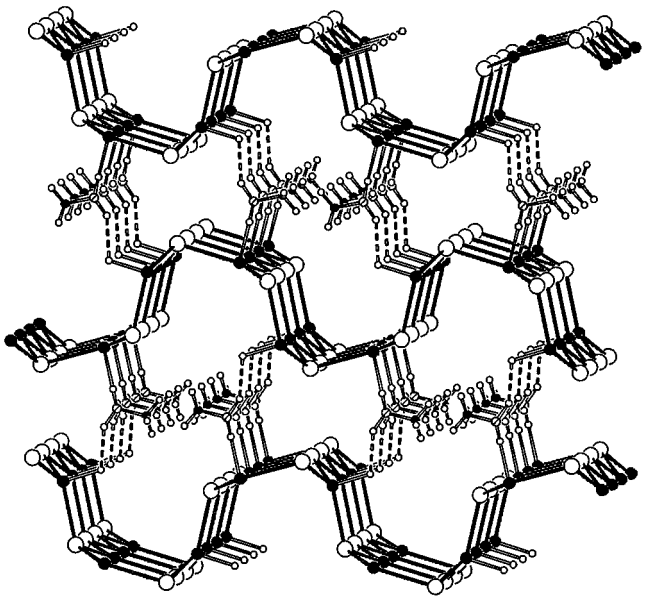

FIG. 6. The schematized 3D network of **2,** formed by the hydrogen bonds joining the [Ag(hmt)] layers via Ag–(H_2O)···(triflate)–Ag bridges. The free triflate anions and solvated water molecule, that fill the channels, are omitted for clarity.

illustrated in Fig. 9. This topology was classified by Wells as the Archimedian binodal 3D net ($8^2$10)-b (23b). We have recently found the same topology in the species [Cu(μ_3-TCNB)(THF)](PF_6) (TCNB = 1,2,4,5-tetracyanobenzene) (6c).

Comments on the structural and topological properties of the Ag–hmt systems. Many Ag–hmt species have been reported in the literature, especially in recent times, and are listed in Table 6. These exhibit a variety of structural types, which are schematically illustrated in Scheme 2, that include a finite cage, a polymeric ribbon, three types of 2D layers and different examples of 3D networks, all noninterpenetrated. A comparison of all these results can enlighten some

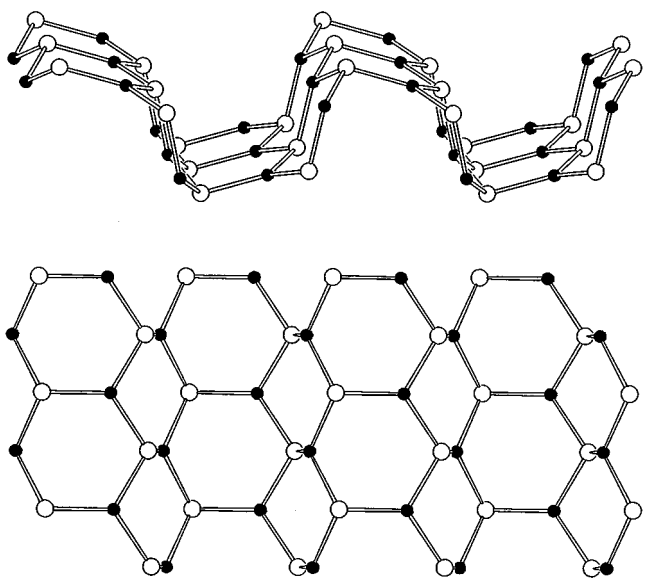

FIG. 5. Schematic representation of the layers of **2,** in two mutually perpendicular directions (solid small spheres, Ag(I); empty big spheres, baricenters of the hmt molecules, here and in the following figures).

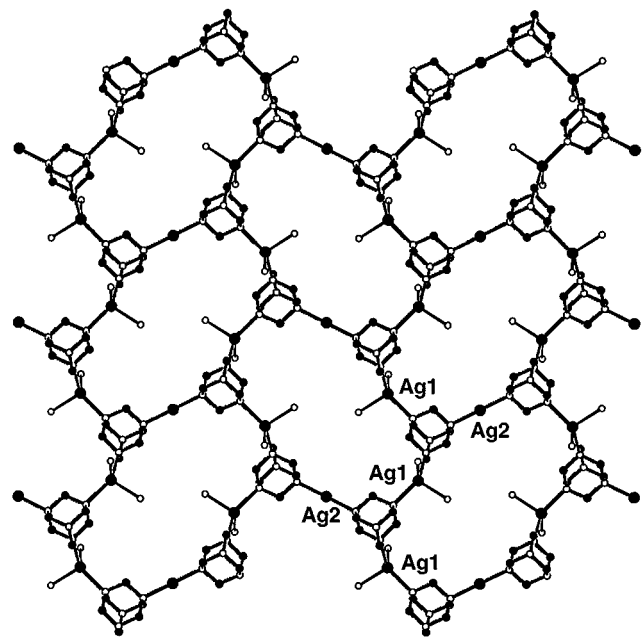

FIG. 7. A single hexagonal layer in compound **3**. The Ag(1) ions form helical chains extending in the [0 1 0] direction.

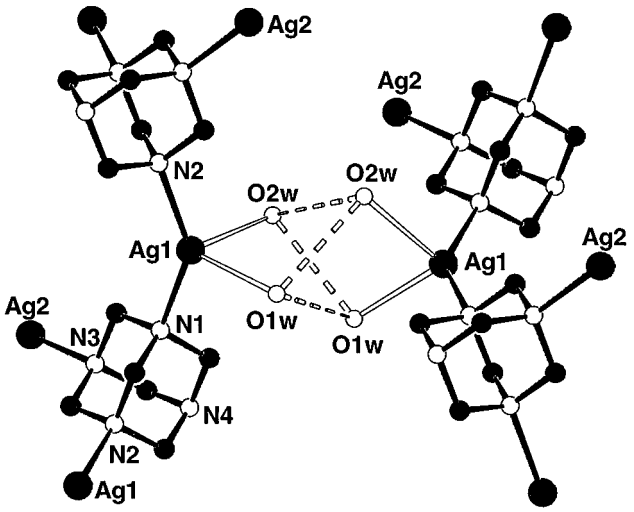

FIG. 8. The hydrogen bond bridge joining different layers of **3**. A partial atom numbering is given.

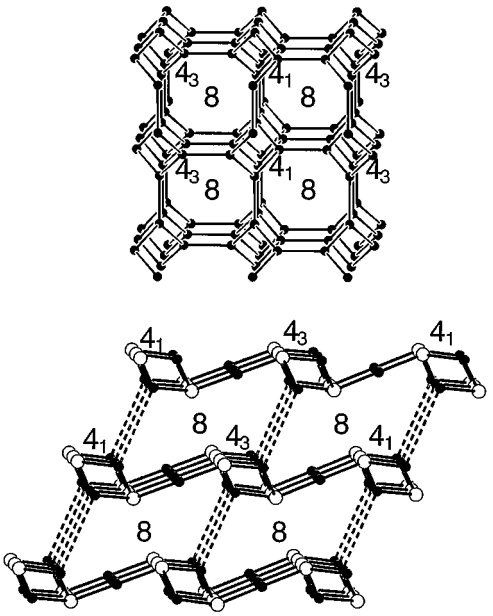

FIG. 9. The ideal ($8^2$10)-b network (top) and the schematic 3D frame formed by hydrogen bonds (dotted lines) in compound **3** (bottom).

common structural properties and can be helpful for a rationalization of the self-assembly processes. We are particularly interested to those species that contain poorly coordinating anions, being not directly involved in networking, but either free or weakly bonded, without topological relevance. This is not the case for the last three species (*n*–*p*), which will not be discussed in detail. We have included in Scheme 2 only the 3D frame of compound *n*, which is sustained by Ag(μ-$MeCO_2$)$_2$Ag bridges (dotted lines), because of its interesting topology.

The list of Table 6 shows that different stable frames are obtained on varying the counterion and/or the Ag/hmt ratio. For example, with $AgPF_6$ five different species have been isolated, exhibiting Ag/hmt ratios in the range from 0.833 : 1 to 1.8 : 1, that illustrate the complex nature of the reaction processes. Other salts that have allowed the isolation of more than one product are $AgNO_3$ and $AgClO_4$.

TABLE 6
The Structurally Characterized Ag-hmt Polymeric Species

Compound	Network[a]	Ag2C[b]	Ag/hmt	Ref.
a [Ag(μ_3-hmt)](NO_3)	2D hexagons	0	1/1	24
b [Ag_2(μ_4-hmt)(NO_3)$_2$]	3D (6^5,8) $CdSO_4$	2	2/1	25
c [Ag(μ_3-hmt)](ClO_4)	2D hexagons	0	1/1	17
d [Ag_3(μ_4-hmt)$_2$(H_2O)$_2$](ClO_4)$_3$	3D (6^3)(6^5,8)-b InS	1	1.5/1	17
e [Ag_5(μ_2-hmt)$_6$](PF_6)$\cdot$ 3CH_2Cl_2	0D D_{3h} cage	3	0.83/1	16
f [Ag(μ_3-hmt)](PF_6)$\cdot$ H_2O	3D (10^3-a) $SrSi_2$	0	1/1	14
g [Ag_4(μ_3-hmt)$_3$(H_2O)](PF_6)$_4\cdot$ 3EtOH	3D ($6,10^2$)$_3$(10^3)	3	1.33/1	16
h [Ag_3(μ_3-hmt)$_2$(H_2O)$_4$](PF_6)$_3$	2D hexagons	3	1.5/1	This work
i [Ag_{11}(μ_4-hmt)$_6$(H_2O)$_{10}$](PF_6)$_{11}\cdot$ 4H_2O	3D 3,4-C	3	1.8/1	15
j [Ag_2(μ_4-hmt)(SO_4)(H_2O)]$\cdot$ 4H_2O	2D squares	2	2/1	22
k [Ag_2(μ_2-hmt)(μ_3-hmt)(H_2O)(SbF_6)]	1D ribbons	1	1/1	15
l [Ag_2(μ_3-hmt)$_2$(CF_3SO_3)(H_2O)](CF_3SO_3)$\cdot$ H_2O	2D hexagons	0	1/1	This work
m [Ag_2(μ_4-hmt)(Tos)$_2$]	2D squares	2	2/1	This work
n [Ag_2(μ_4-hmt)(O_2CCH_3)](CH_3CO_2)$\cdot$ 4.5H_2O	3D (6^3)(6^5,8) new	1	2/1	22
o [Ag_4(μ_4-hmt)Cl_4]	3D complex	0	4/1	26
p [Ag_4(μ_4-hmt)Br_4][c]	3D complex	0	4/1	27

[a] Only the coordinative bonds are considered.
[b] Number of biconnected silver atoms per formula unit.
[c] Isomorphous with the chlorine analog.

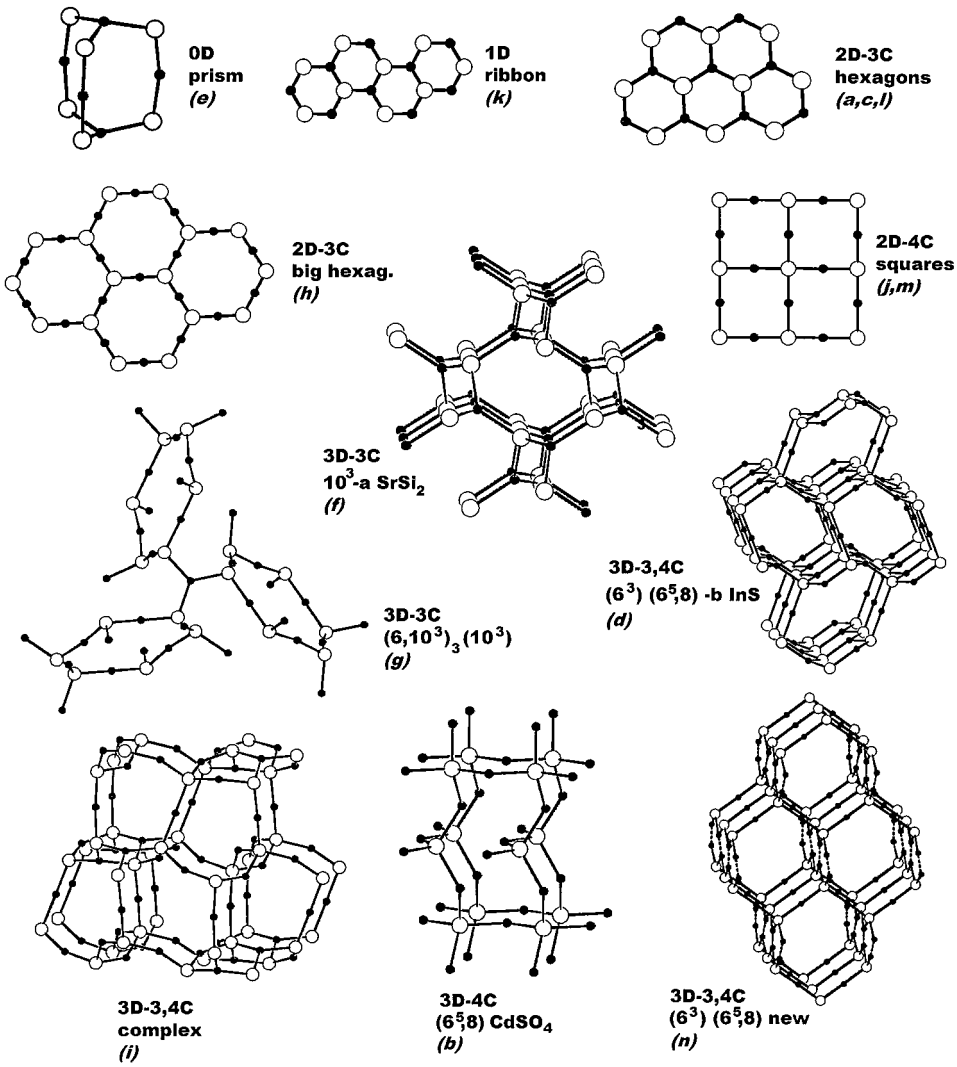

SCHEME 2

These two salts give 1 : 1 adducts (a and c) that contain quite similar 2D hexagonal layers, while in the presence of an excess of silver ions, 3D frameworks with hmt ligands, all four-connected, are recovered in both cases (b and d), but showing a different stoichiometry. The equimolar Ag/hmt step seems less influenced by the anion (see also the case of the triflate, l), probably because the 2D layers obtained present interlayer regions that can accomodate with poor selectivity the counterions. Note, however, that an Ag/hmt ratio of 1 : 1 does not ensure the formation of a 2D layered polymer, as shown by the 1D ribbon structure of *k* and the 3D frame of f (both containing additional solvated water molecules).

Table 6 shows that hmt acts as a tetradentate ligand in 50% of the cases and that it plays in all the networks the role of a node, while the silver ions are often only spacers. This confirms that the choice of target structural motifs like II and IV of Scheme 1 in the engineering of these polymers is reasonable, and, in fact, compound **3** contains type II extended layers. On the other hand, the 2D nets of j and m and the 3D frame of b were rather unpredictable, being their reference topological types associated to the presence of square planar, rather than tetrahedral, centers (see Scheme 2). Indeed, many square grid layers have been assembled by using pseudo-square planar metal centers with linear bidentate rod-like ligands, and a 3D (interpenetrated) network of the $CdSO_4$ topology (like b) has been recently reported, containing Cu(II) pseudo-square planar centers and the rigid spacer ligands bis(4-pyridyl)ethene (28). Structures like those of j, m, and b can be obtained thanks only to the versatility of the silver ions, which can assume coordination geometries spanning *with continuity* all the situations, from the ideal digonal, to the trigonal, to the tetrahedral one. The observed deviations from linearity are due to the (rather

weak) interactions of the Ag(I) ions with the anions or solvent molecules, that, though they do not have a topological role, seem to be of fundamental importance in orienting the formation of the polymeric array.

Many of the Ag–hmt systems contain as constituting units the basic hexagons of I or II in Scheme 1, but no example of the superdiamond nets III or IV has been observed. Compounds having the correct [Ag(hmt)] stoichiometry for giving III (a, c, f, k, and l) show the preference for 2D or 3D structures with lower connectivity (all three-connected). This is very probably due to the fact that the adamantanoid cages of III (with edges of 3.7–3.9 Å) are too small to contain the counterions, as we have already outlined on discussing the structure of f (Scheme 2), that can be ideally derived by III on breaking a specific set of Ag–N bonds. The lack of a structure like the diamondoid IV (with ideal edges of ca. 7.6 Å) in the three cases showing the right $[Ag_2(hmt)]$ composition (b, j, and m) can be in part explained taking into account the above-mentioned deviations from linearity of the hmt–Ag–hmt bridges. Note, however, that the network in compound d represents a sort of intermediate situation between III and IV, containing hexagonal layers (I) that are not directly superimposed (as in III) but are connected via Ag(I) spacers.

Taking into account that subtle factors can drive the self-assembly processes of these Ag–hmt systems into different directions, the obtainement of new types of networks (possibly also of IV) cannot be ruled out on further changing the reaction conditions.

REFERENCES

1. (a) B. F. Hoskins and R. Robson, *J. Am. Chem. Soc.* **112,** 1546 (1990); (b) R. Robson, B. F. Abrahams, S. R. Batten, R. W. Gable, B. F. Hoskins, and J. Liu, "Supramolecular Architecture," Chap. 19, ACS, Washington, DC, 1992; (c) S. R. Batten and R. Robson, *Angew. Chem., Int. Ed. Engl.* **37,** 1460 (1998); (d) M. J. Zaworotko, *Chem. Soc. Rev.* 283 (1994); (e) C. L. Bowes and G. A. Ozin, *Adv. Mater.* **8,** 13 (1996); (f) O. M. Yaghi, H. Li, C. Davis, D. Richardson, and T. L. Groy, *Acc. Chem. Res.* **31,** 474 (1998); (g) M. Munakata, L. P. Wu, and T. Kuroda-Sowa, *Adv. Inorg. Chem.* **46,** 173 (1999); (h) A. J. Blake, N. R. Champness, P. Hubberstey, W. S. Li, M. A. Withersby, and M. Schroder, *Coord. Chem. Rev.* **183,** 117 (1999); (i) C. B. Aakeröy, *Acta Crystallogr. B* **53,** 569 (1997).
2. Recent papers on this subject are: (a) A. J. Blake, N. R. Champness, S. S. M. Chung, W. S: Li, and M. Schroder, *Chem. Commun.* 1005 (1997); (b) D. Hagrman, R. P. Hammond, R. Haushalter, and J. Zubieta, *Chem. Mater.* **10,** 2091 (1998); (c) L. Carlucci, G. Ciani, P. Macchi, and D. M. Proserpio, *Chem. Commun.* 1837 (1998); (d) K. A. Hirsch, S. R. Wilson, and J. S. Moore, *Chem. Commun.* 13 (1998); (e) B. F. Abrahams, P. A. Jackson, and R. Robson, *Angew. Chem., Int. Ed. Engl.* **37,** 2656 (1998); (f) H.-P. Wu, C. Janiak, G. Rheinwald, and H. Lang, *J. Chem. Soc. Dalton Trans.* 183 (1999); (g) H. Gudbjartson, K. Biradha, K. M. Poirier, and M. J. Zaworotko, *J. Am. Chem. Soc.* **121,** 2599 (1999).
3. Recent papers on this subject are: (a) T. M. Reineke, M. Eddaoudi, M. Fehr, D. Kelly, and O. M. Yaghi, *J. Am. Chem. Soc.* **121,** 1651 (1999); (b) T. M. Reineke, M. Eddaoudi, M. O'Keeffe, and O. M. Yaghi, *Angew. Chem., Int. Ed. Engl.* **38,** 2590 (1999); (c) O. R. Evans, Z. Wang. R.-G. Xiong, B. M. Foxman, and W. Lin, *Inorg. Chem.* **38,** 2969 (1999).
4. (a) C. B. Aakeröy, A. M. Beatty, and D. S. Leiden, *Angew. Chem., Int. Ed. Engl.* **38,** 1815 (1999); (b) C. B. Aakeröy and A. M. Beatty, *J. Mol. Struct.* **474,** 91 (1999).
5. (a) B. F. Abrahams, S. R. Batten, H. Hamit, B. F. Hoskins, and R. Robson, *J. Chem. Soc. Chem. Commun.* 1313 (1996); (b) B. F. Abrahams, S. R. Batten, M. J. Grannas, H. Hamit, B. F. Hoskins, and R. Robson, *Angew. Chem., Int. Ed. Engl.* **38,** 1475 (1999); (c) G. B. Gardner, D. Venkataraman, J. S. Moore, and S. Lee, *Science* **374,** 792 (1995); (d) D. Venkataraman, S. Lee, J. S. Moore, P. Zhang, K. A. Hirsch, G. B. Gardner, A. C. Covey, and C. L. Prentice, *Chem. Mater.* **8,** 2030 (1996); (e) D. M. L. Goodgame, D. A. Grachvogel, and D. J. Williams, *Angew. Chem., Int. Ed. Engl.* **38,** 153 (1999).
6. (a) B. F. Abrahams, B. F. Hoskins, D. M. Michail, and R. Robson *Nature* (*London*) **369,** 727 (1994); (b) L. Shields, *J. Chem. Soc. Faraday Trans.* **81,** 1 (1985); (c) L. Carlucci, G. Ciani, D. W. v. Gudenberg, and D. M. Proserpio, *New J. Chem.* **23,** 397 (1999).
7. (a) F.-Q. Liu and T. D. Tilley, *Inorg. Chem.* **36,** 5090 (1997); (b) W. Choe, Y.-H. Kiang, Z. Xu, and S. Lee, *Chem. Mater.* **11,** 1776 (1999).
8. Two examples of 3D networks joined by metal spacers are reported in: (a) B. F. Abrahams, B. F. Hoskins, and R. Robson, *J. Am. Chem. Soc.* **113,** 3606 (1991); (b) K. Inoue, T. Hayamizu, H. Iwamura, D. Hashizume, and Y. Ohashi, *J. Am. Chem. Soc.* **118,** 1803 (1996).
9. G. R. Desiraju, *Angew. Chem., Int. Ed. Engl.* **34,** 2311 (1995).
10. O. Ermer, *J. Am. Chem. Soc.* **110,** 3747 (1988).
11. O. M. Yaghi, Z. Sun, D. Richardson, and T. L. Groy, *J. Am. Chem. Soc.* **116,** 807 (1994).
12. K. Tam, A. Darovsky, and J. B. Parise, *J. Am. Chem. Soc.* **117,** 7039 (1995).
13. O. Ermer, *J. Chem. Soc. Perkin Trans.* **2,** 925 (1994).
14. L. Carlucci, G. Ciani, D. M. Proserpio, and A. Sironi, *J. Am. Chem. Soc.* **117,** 12861 (1995).
15. M. Bertelli, L. Carlucci, G. Ciani, D. M. Proserpio, and A. Sironi, *J. Mater. Chem.* **7,** 1271 (1997).
16. L. Carlucci, G. Ciani, D. M. Proserpio, and A. Sironi, *Inorg. Chem.* **36,** 1736 (1997).
17. L. Carlucci, G. Ciani, D. W. v. Gudenberg, D. M. Proserpio, and A. Sironi, *Chem. Commun.* 631 (1997).
18. A. Altomare, M. C. Burla, M. Camalli, G. Cascarano, C. Giacovazzo, A. Guagliardi, A. Moliterni, G. Polidori, and R. Spagna, *J. Appl. Crystallogr.* **32,** 115 (1999).
19. G. M. Sheldrick, "SHELX-97: Program for Structure Refinement," Univ. of Goettingen, Germany, 1997.
20. E. Keller, "SCHAKAL 97: A Computer Program for the Graphical Representation of Crystallographic Models," Univ. of Freiburg, Germany, 1997.
21. See, e.g., (a) M. Munakata, L. P. Wu, T. Kuroda-Sowa, M. Maekawa, Y. Suenaga, G. L. Ning, and T. Kojima, *J. Am. Chem. Soc.* **120,** 8610 (1998); (b) G. L. Ning, M. Munakata, L. P. Wu, M. Maekawa, T. Kuroda-Sowa, Y. Suenaga, and K. Sugimoto, *Inorg. Chem.* **38,** 1376 (1999).
22. M.-L. Tong, S.-L. Zheng, and X.-M. Chen, *Chem. Commun.* 561 (1999).
23. (a) A. F. Wells, "Structural Inorganic Chemistry," 5th ed. Oxford Univ. Press, Oxford, 1984; (b) A. F. Wells, "Further Studies of Three-Dimensional Nets," ACA Monograph 8. 1979.
24. A. Michelet, B. Voissat, P. Khodadad, and N. Rodier, *Acta Crystallogr. B* **37,** 2171 (1981).
25. O. M. Yaghi, H. Li, and M. O'Keeffe, *Mater. Res. Soc. Symp. Proc.* **453,** 127 (1997).
26. T. C. W. Mak, *Inorg. Chim. Acta* **84,** 19 (1984).
27. T. C. W. Mak, *Jiegou Huaxue* (*J. Struct. Chem.*) **4,** 16 (1985).
28. K. N. Power, T. L. Hennigar, and M. J. Zaworotko, *Chem. Commun.* 595 (1998).